Carbon Dioxide Capture from Synthesis Gas Containing Steam by Pressure Swing Adsorption at Mid-high Temperature

Cheng-tung Chou[1]*, Yu-Hau Shih [1], Yu-Jie Huang[1] and Hong-sung Yang[2]
[1]*Department of Chemical and Materials Engineering, National Central University, Jhong-Li, Taiwan*
[2]*Center for General Education, Hwa-Hsia Institute of Technology, New Taipei City, Taiwan*

Keywords: Pressure Swing Adsorption, CO_2 Capture, Synthesis Gas.

Abstract: Global warming has become more and more serious, which is caused by greenhouse gases. Therefore, decreasing the emission of CO_2 has become an important research topic in the world. This study aimed to utilize a pressure swing adsorption (PSA) process to capture CO_2 from synthesis gas, which is the effluent stream of water-gas-shift reactor. The PSA process studied is a single-bed four-step process at mid-high temperature using K_2CO_3-promoted hydrotalcite. The feed gas entering the PSA process consists of 27 % H_2O, 5 % CO, 28 % CO_2 and 40 % H_2. It uses the method of lines combined with upwind differences, cubic spline approximation and LSODE of ODEPACK software to solve the equations. The optimal operating condition is obtained by varying the operating variables, such as feed pressure, bed length, etc. Furthermore, single-bed four-step process could achieve 98.49% recovery of H_2 as the top product and 96.42% purity and 96.57% recovery of CO_2 as the bottom product.

1 INTRODUCTION

Carbon dioxide is considered to be one of the major greenhouse gases that is directly influencing the global climate changes. The United Nations Intergovernmental Panel on Climate Change (IPCC) has studied these problems and a general conclusion has been achieved between researchers, industry leaders, and politicians that dramatic reduction in greenhouse gas emissions must be achieved in order to stop climatic changes (IPCC, 2005); (Abu-Zahra et al., 2009). So using coal more efficiently and turning it into a clean energy source is an important issue for the whole world. An integrated gasification combined cycle (IGCC) is a potential electric power technology that turns coal into synthesis gas, which can be burned to generate power.

The CO composition in syngas reacts with steam to generate CO_2 and H_2 via the water-gas-shift reaction, $CO + H_2O \rightarrow CO_2 + H_2$. In this study, pressure swing adsorption (PSA) is utilized to capture CO_2 from the effluent stream of water-gas-shift reaction at mid-high temperature, and the purified H_2 can be sent to gas turbine for generating electrical power or can be used for other energy source. This technology consists of gas adsorption at high pressure and desorption at low pressure to produce high-purity products. Conventionally, PSA is used to separate CO_2 and H_2 at ambient temperature. For traditional physical adsorbent, such as zeolite and activated carbon, the adsorbed amount of CO_2 is too low to separate CO_2/H_2 at mid-high temperature. Because the outlet stream from water-gas-shift reactor is already at nearly 400^{o}C, in order to avoid separating CO_2 and H_2 at ambient temperature, and later raise the temperature of H_2 for power generation, which will cause energy waste, in this study PSA processes with K_2CO_3-promoted hydrotalcite adsorbent are studied to capture CO_2 from the outlet stream of water-gas-shift reactor at 400^{o}C. According to literature (Lee et al., 2007a), K_2CO_3-promoted hydrotalcite is a chemisorbent that adsorbs CO_2 at mid-high temperature and it does not adsorb other gases, such as CO, H_2 and H_2O. As required by the U.S. Department of Energy, it is important to be able to concentrate the captured CO_2 into >90 % concentration that is suitable for underground storage.

The feed gas entering the PSA process consists of CO, CO_2, H_2 and H_2O according to National Energy Technology Laboratory report (NETL, 2009).

Most PSA papers assume that steam is removed before entering CO_2-capture PSA process. In this

Chou C., Shih Y., Huang Y. and Yang H..
Carbon Dioxide Capture from Synthesis Gas Containing Steam by Pressure Swing Adsorption at Mid-high Temperature .
DOI: 10.5220/0004624705290536
In *Proceedings of the 3rd International Conference on Simulation and Modeling Methodologies, Technologies and Applications* (MSCCEC-2013), pages 529-536
ISBN: 978-989-8565-69-3

study we intend to consider the steam composition in feed gas into PSA process for real-case study.

2 METHODOLOGY

2.1 Mathematical Modelling

In the non-isothermal dynamic model, the following assumptions are made:

1. The linear driving force model is used because mass transfer resistance between the gas phase and solid phase exists.
2. Only CO_2 is adsorbed in K_2CO_3-promoted hydrotalcite.
3. The ideal gas law is applicable.
4. Adiabatic system.
5. Only axial concentration and temperature gradient are considered.
6. The pressure drop along the bed can be neglected due to large particle size.

These assumptions are used in the following equations:

Overall mass balance:

$$-\frac{\partial q}{\partial z}=\frac{\varepsilon A}{R}\frac{\partial(P/T)}{\partial t}+(1-\varepsilon)A\sum_{i=1}^{n}\frac{\partial n_i}{\partial t} \quad (1)$$

Mass balance for component *i:*

$$\frac{\partial}{\partial z}\left(\frac{\varepsilon AD_{ax,i}P}{RT}\frac{\partial y_i}{\partial z}\right)-\frac{\partial(y_i q)}{\partial z}=\frac{\varepsilon A}{R}\frac{\partial}{\partial t}\left(\frac{y_i P}{T}\right)+(1-\varepsilon)A\frac{\partial n_i}{\partial t} \quad (2)$$

Energy balance:

$$\begin{aligned}&\left(A\bar{k}\right)\frac{\partial^2 T}{\partial z^2}-\frac{\partial}{\partial z}\left(\bar{C}_p qT\right)-\pi Dh\left(T-T_\infty\right)\\&=\frac{\varepsilon A}{R}\frac{\partial}{\partial t}\left(\bar{C}_p P\right)+(1-\varepsilon)A\sum_{i=1}^{n}\frac{\partial}{\partial t}\left[n_i\left(\tilde{C}_{pi}T-H_i\right)\right]+(1-\varepsilon)\rho_s\hat{C}_{ps}A\frac{\partial T}{\partial t}\end{aligned} \quad (3)$$

Linear driving force model:

$$\frac{\partial N_i}{\partial t}=K_{LDF}\left(N_i^*-N_i\right) \quad (4)$$

The adiabatic system means that there is no heat transfer between bed and surrounding so that h = 0 in Eq. (3).

Boundary conditions can be assumed as follows: At the inlet end:

$$c(\mathrm{t},0)=c_{in}(\mathrm{t})\ ,T(\mathrm{t},0)=T_{in}(t) \quad (5)$$

At the outlet end:

$$\frac{\partial \mathrm{c(t,L)}}{\partial \mathrm{z}}=0\ ,\frac{\partial \mathrm{T(t,L)}}{\partial \mathrm{Z}}=0 \quad (6)$$

The flow rates at the two ends of the bed are estimated by using the valve equation recommended by Fluid Controls Institute Inc.:

$$\mathrm{q'}=16.05C_v\sqrt{\frac{(P_1^2-P_2^2)}{SG\times T}} \quad \text{for } P_2>0.53P_1 \quad (7)$$

$$\mathrm{q'}=13.61C_vP_1\sqrt{\frac{1}{SG\times T}} \quad \text{for } P_2\le 0.53P_1 \quad (8)$$

Twenty-one basic grid points are marked in the bed to set up the initial concentration, initial temperature, and initial pressure. The partial differential equations are converted to ordinary differential equations by the method of lines. The spatial derivatives of the concentration and the gas temperature are evaluated by upwind differences at every grid point. The cubic spline approximation is used to estimate the flow rates in the adsorptive bed. The concentration, temperature, and adsorption quantity in the bed are integrated with respect to time by LSODE of ODEPACK software with a time step of 0.1s. The simulation is stopped by using Eq. 9 when the system reaches a cyclic steady state.

$$\sum(1-\frac{\mathrm{Y(last\ cycle)}}{\mathrm{Y(this\ cycle)}})^2<1\times10^{-4} \quad (9)$$

2.2 PSA Process

The PSA process studied is a single-bed four-step process at mid-high temperature using K_2CO_3-promoted hydrotalcite. The feed gas is from the effluent stream in the water-gas-shift reactor which is cited in the report of National Energy Technology Laboratory (NETL, 2009). The feed gas entering the PSA process consists of 27 % H_2O, 5 % CO, 28% CO_2 and 40 % H_2. The process is described as follows: feed pressurization (I), high pressure adsorption (II), cocurrent depressurization (III), vacuum desorption (IV). During step (I), the bed pressure increases from atmospheric pressure to high pressure, and less-adsorbed products are produced. Strongly adsorptive carbon dioxide is produced during step (IV) when the bed pressure decreases from high pressure to low pressure (0.1 atm). The procedure of the sing-bed four-step process is shown in Figure 1. The step time and the physical parameters of adsorption bed are shown in Tables 1 and 2.

Table 1: Step time for single-bed four-step process.

(I)	10s
(II)	39s
(III)	10s
(IV)	39s

Table 2: Physical parameters of bed.

Bed length(cm)	100
Bed diameter(cm)	100
Bed volume(L)	784
Adsorbent density(g/cm^3)	1.563[#]
Adsorbent heat capacity(J/g.K)	0.85[#]
Bed void	0.37
Operating temperature(K)	673.14
Feed pressure(atm)	25
Vacuum pressure(atm)	0.1

[#]Ding and Alpay, 2000

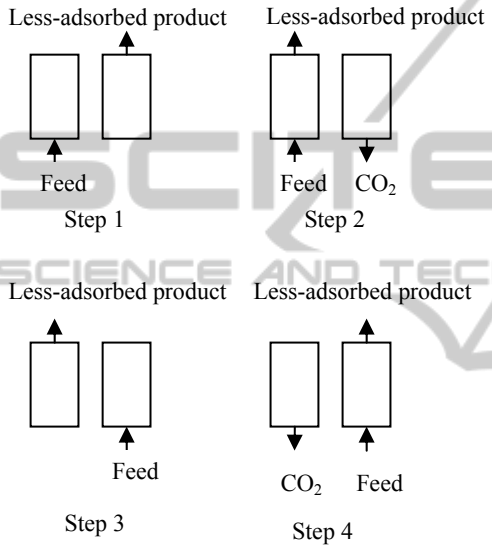

Figure 1: Procedure of single-bed four-step PSA process

Isotherm of K_2CO_3-promoted hydrotalcite was measured at 400°C in the pressure range of 0-3atm by Lee et al. (2007a) and shown in Figure 2. The figure also shows the best fit of the CO_2 chemisorption isotherms using the following Eq. (10). The parameters of model for sorption of CO_2 are given in Table 3.

Table 3: Parameters of model for sorption of CO_2 on K_2CO_3-promoted hydrotalcite.

m(mole/kg)	0.25
a	2.5
q_c(J/mole)	$2.098*10^4$
ΔH_R(J/mole)	$4.210*10^4$
k_c(atm^{-1})	37.4
k_R(atm^{-a})	2.5

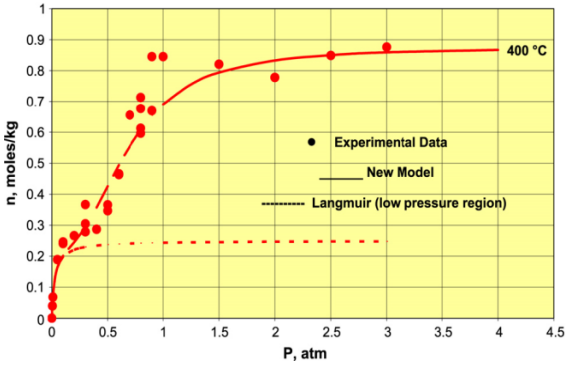

Figure 2: CO_2 chemisorption isotherm on K_2CO_3-promoted hydrotalcite at 400 ◦C (Lee et al., 2007a).

$$n_i^*(P,T) = \frac{mK_CP[1+(a+1)K_RP^a]}{[1+K_CP+K_CK_RP^{(a+1)}]} \quad (10)$$

$$K_C = K_{C0}\exp(\frac{q_c}{RT}) \quad (11)$$

$$K_R = K_{R0}\exp(\frac{\Delta H_R}{RT}) \quad (12)$$

3 RESULTS AND DISCUSSION

3.1 Simulation Verification

The breakthrough curve studied by Lee et al. (2007a) was used to verify the simulation program. Different compositions of CO_2 + N_2 mixtures were used as the feed gas.The operating conditions used are given in Table 4. The results are shown in Figures 3 and 4. It shows that the simulation results are very close to experiment data. Therefore, the simulation program can be trusted.

Table 4: Operating parameters of breakthrough curve simulation.

Operating pressure(atm)	1
Operating temperature(K)	673.14
Feed flow rate(L/min)	$5.0*10^{-3}$
Bed length(cm)	101.6
Bed diameter(cm)	1.73
Bed volume(L)	0.238
Bulk density(g/cm^3)	0.82
Adsorption Time Constant (min^{-1})	3.0
Feed composition	(40% CO_2 , 60% N_2) (50% CO_2 , 50% N_2) (60% CO_2 , 40% N_2)

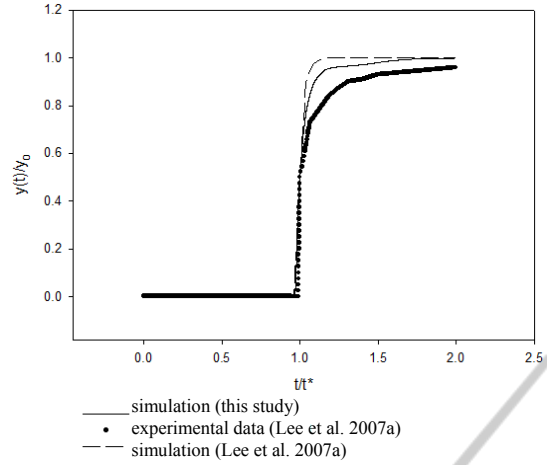

Figure 3: Simulation of breakthrough curve (inlet CO_2 mole fraction=0.4) .

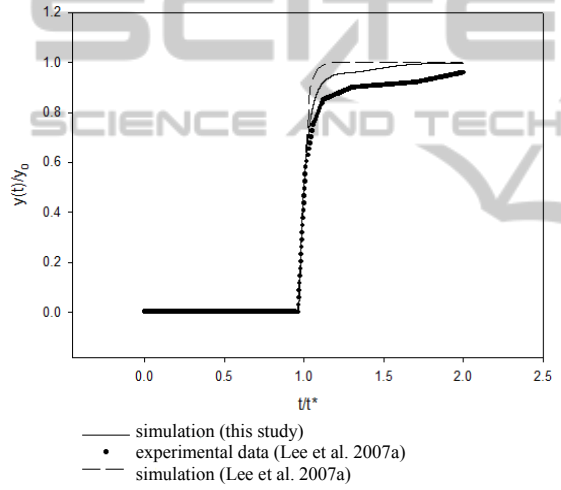

Figure 4: Simulation of breakthrough curve (inlet CO_2 mole fraction=0.5).

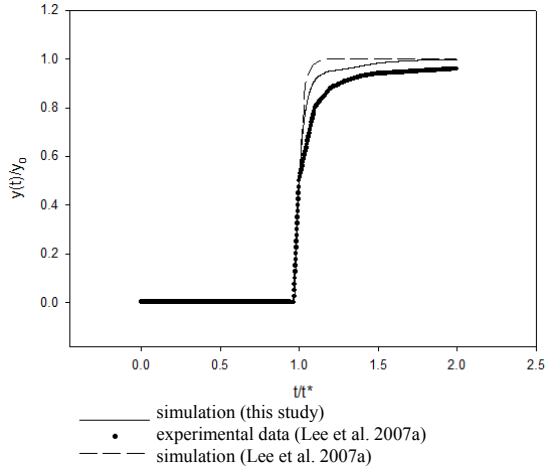

Figure 5: Simulation of breakthrough curve (inlet CO_2 mole fraction=0.6).

The desorption curve studied by Lee et al. (2007b) was also compared to our simulation. Figure 6 shows the column dynamic data (fraction of CO_2 desorbed as a function of inlet N_2 purge gas quantity) for desorption of 40% CO_2 +N_2 by N_2 purge. The operating conditions used are given in Table 5. The agreement between our simulation and the experimental data is pretty good.

Table 5: Operating parameters of desorption curve simulation.

Operating pressure(atm)	1
Operating temperature(K)	793.14
Feed flow rate(L/min)	6.667×10^{-3}
Bed length(cm)	100
Bed diameter(cm)	1.73
Bed volume(L)	0.23882
Bulk density(g/cm^3)	0.82
Initial gas phase concentration	40%CO_2/N_2

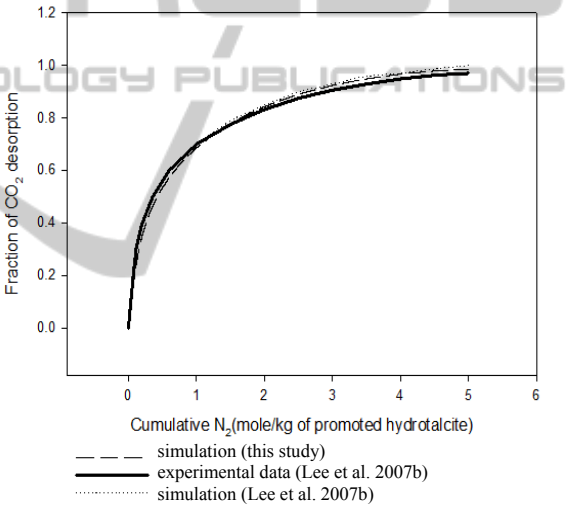

Figure 6: Simulation of desorption curve.

3.2 Single-Bed Four-step PSA Process Simulation

In this study, the optimal operating conditions are discussed by varying the operating variables, such as feed pressure, bed length, vacuum pressure, feed flow rate, high pressure adsorption time and vacuum desorption time.

Definition of the recovery is:

$$\text{Recovery} = \frac{\text{product flow per cycle} \times \text{product concentration feed}}{\text{flow per cycle} \times \text{feed concentration}}$$

3.2.1 Feed Pressure

All the operating variables such as vacuum pressure,

bed length, feed rate and step time are fixed, except for feed pressure. Because the amount of gas adsorbed on K_2CO_3-promoted hydrotalcite increases as feed pressure increases, the flow of the strong adsorptive component to the bottom of the bed during desorption increases. Figure 7 shows that as feed pressure increases, the CO_2 purity and recovery in bottom product increases because CO_2 adsorption quantity becomes larger.

Figure 8 shows that the mole fraction of CO_2 which does not change too much with different feed pressure after cocurrent depressurization step. Therefore weak adsorptive component recovery doesn't vary in top product.

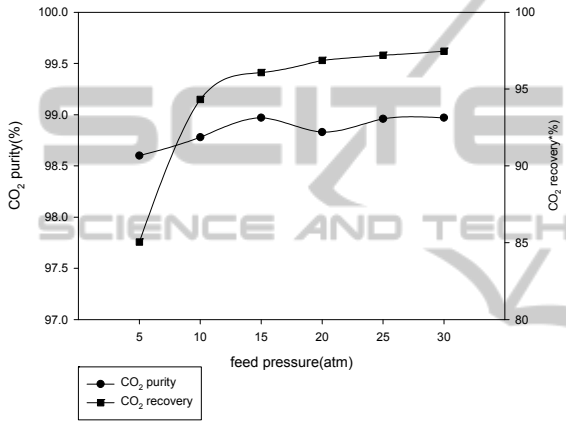

Figure 7: Effect of feed pressure on CO_2 in bottom product.

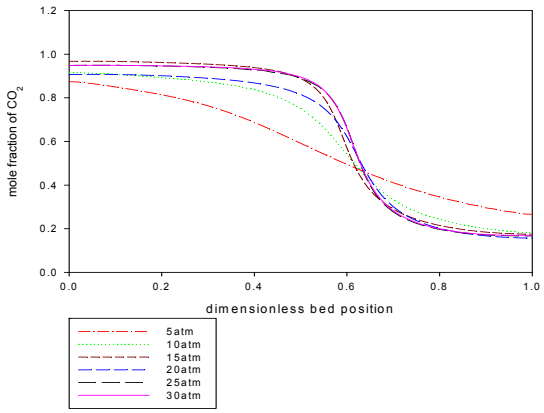

Figure 8: Mole fraction of CO_2 after concurrent depressurization step.

3.2.2 Bed Length

All the operating variables are fixed except bed length. With increasing bed length, the amount of adsorbent and the amount of adsorbed gas increase. Figure 9 shows that as bed length decreases, the CO_2 purity increases due to that the amount of CO_2 flow to the top product increases. At the same feed flow rate CO_2 recovery decreases due to that the amount of CO_2 flow to the top product increases.

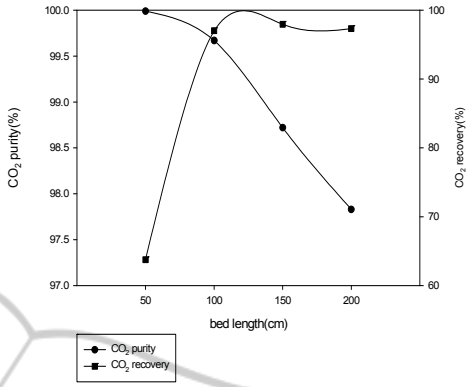

Figure 9: Effect of bed length on CO_2 in bottom product.

3.2.3 Vacuum Pressure

All the operating variables are fixed except vacuum pressure. As the vacuum pressure increases, the

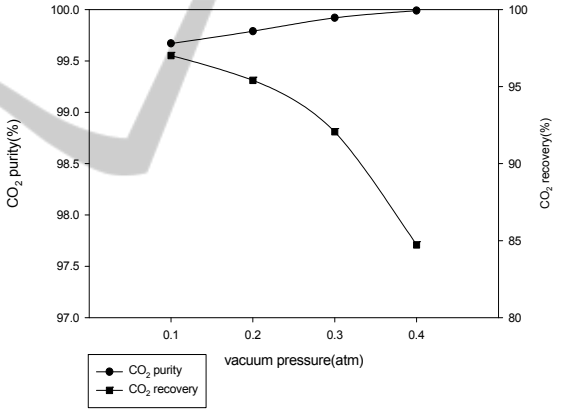

Figure 10: Effect of bed length on CO_2 in bottom product.

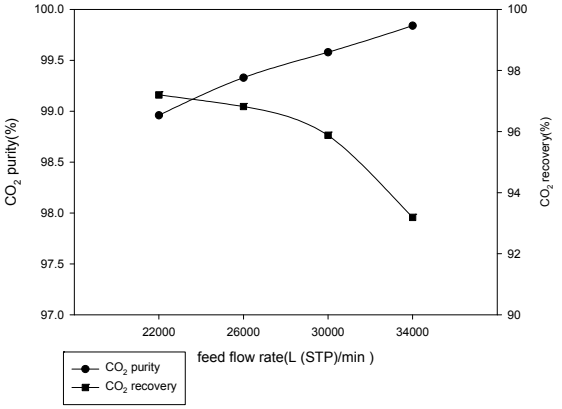

Figure 11: Effect of feed flow rate on CO_2 in bottom product.

amount of desorption gas at desorption step decreases. Figure 10 shows that as the vacuum pressure increases, the CO_2 recovery decreases due to that the amount of adsorbed gas flow to the bottom product at desorption step decreases.

3.2.4 Feed Flow Rate

All the operating variables are fixed except feed flow rate. As the feed flow rate increases, the amount of CO_2 increases at high pressure adsorption step. Figure 11 shows that as the feed flow rate increases, the CO_2 recovery decrease due to that the amount of adsorption/desorption are approximately fixed. The CO_2 purity increases as the amount of adsorbed gas increases.

3.2.5 High Pressure Adsorption Time and Vacuum Desorption Time

All the operating variables are fixed except high pressure adsorption time/vacuum desorption time. The amount of CO_2 increases in the column as the pressure adsorption time increases. Figures 12 and 13 show that the amount of CO_2 flow to the top product increases with increasing high pressure adsorption time/vacuum desorption time. Therefore, Figure 14 shows that CO_2 recovery decreases with decreasing 2nd/4th step time.

The best operating conditions for the single-bed four-step PSA process at mid-high temperature is shown in Figure 15. The results of best operating condition for the single-bed four-step process at mid-high temperature are 96.42% purity and96.57% recovery of CO_2 as bottom product as shown in Figure 15. Table 6 shows the optimal operating condition for the single-bed four-step process.

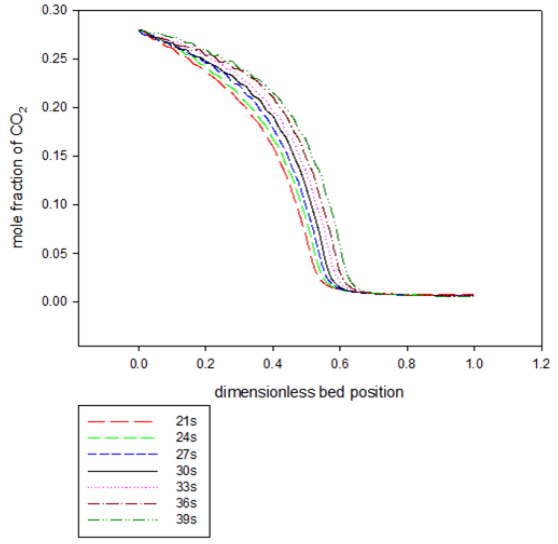

Figure 12: Mole fraction of CO_2 after high pressure adsorption step at different high pressure adsorption time /vacuum desorption time.

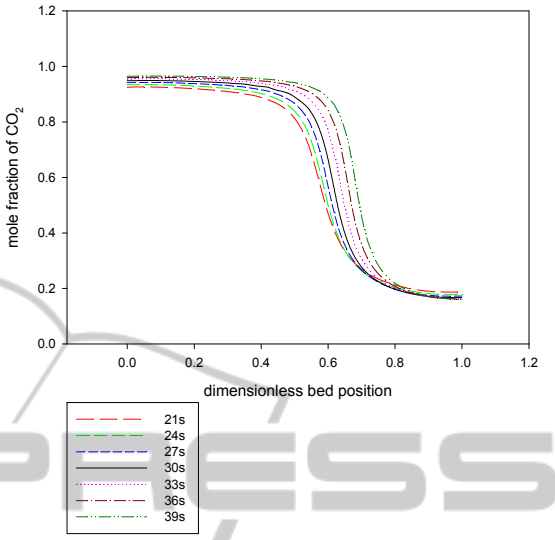

Figure 13: Mole fraction of CO_2 after vacuum desorption step at different high pressure adsorption time/vacuum desorption time.

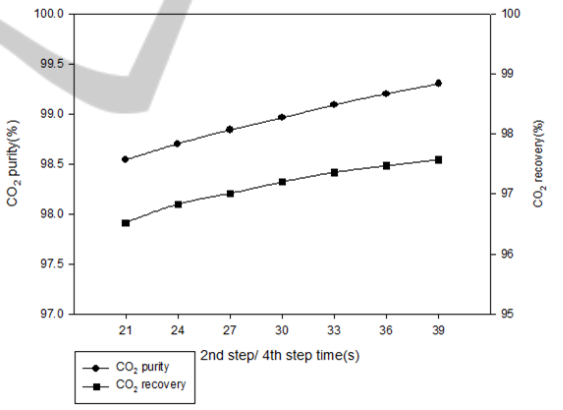

Figure 14: Effect of 2nd/4th step time on CO_2 in bottom product.

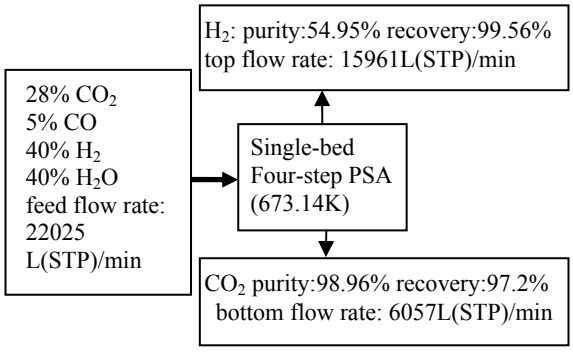

Figure 15: Results of the single-bed four-step PSA process at mid-high temperature.

4 CONCLUSIONS

A single-bed four-step pressure swing adsorption process is explored in this simulation study. The adsorbent K_2CO_3-promoted hydrotalcite was used (Lee et al., 2007a). The accuracy of the simulation program is verified by comparing our simulation results with the experimental data of breakthrough curve and desorption curve from Lee et al. (2007a, 2007b). The optimal operating condition is obtained by varying the operating variables, such as feed pressure, bed length, feed flow rate, etc. Furthermore, the optimal operating condition for inlet (27 % H_2O, 5 % CO, 28 % CO_2 and 40 % H_2) at mid-high temperature 673K and bed diameter 100cm is bed length 200cm, feed pressure 25atm, vacuum pressure 0.1atm and step times at10s, 30s, 10s and 30 s. The best results and the optimal operating condition for the single-bed four-step PSA process at mid-high temperature are shown in Figure 15 and Table 6. In the future, our research will proceed with dealing the top stream from CO_2-PSA by a second stage H_2-PSA to improve H_2 purity.

Table 6: The optimal operating condition for the single-bed four-step process.

operating condition	Feed pressure(atm)	25
	high pressure adsorption time and vacuum desorption time (s)	30
	Vacuum pressure(atm)	0.1
	Feed flow rate L(STP)/min	22000
	Bed length(cm)	200
Simulation result	bottom flow rate L(STP)/min	6187
	CO_2 purity	96.42
	CO_2 recovery	96.57
	top flow rate L(STP)/min	15870
	CO_2 purity	1.34
	CO_2 recovery	3.45
	H_2 purity	54.77
	H_2 recovery	98.49
	CO purity	6.86
	CO recovery	98.69
	H_2O purity	37.02
	H_2O recovery	98.64

ACKNOWLEDGEMENTS

The authors wish to thank the financial support from National Science Council, Taiwan under project number NSC 102-3113-P-008 -007.

REFERENCES

Abu-Zahra M. R. M., Feron P. H. M., Jansens P. J., Goetheer E. L. V., 2009, *New process concepts for CO_2 post-combustion capture process integrated with co-production of hydrogen*, International J. of Hydrogen Energy, 34, 3992-4004.

Ding Y. and Alpay E., 2000, Equilibria and kinetics of CO2 adsorption on hydrotalcite adsorbent, Chemical Engineering Science, 55, 3461-3474.

IPCC (Intergovernmental Panel on Climate Change), 2005, *Carbon dioxide capture and storage*, Cambridge University Press.

Lee K. B., Caram H. S., Verdooren A., Sircar S., 2007a, *Chemisorption of carbon dioxide on potassium carbonate promoted hydrotalcite*, J. of Colloid and Interface Science, 308, 30-39.

Lee K. B., Beaver M. G., Caram H. S., Sircar S., , 2007b, *Reversible chemisorption of carbon dioxide: simultaneous production of fuel-cell grade H_2 and compressed CO_2 from synthesis gas*, Adsorption, vol. 13, pp. 385-392.

NETL (National Energy Technology Laboratory), 2009 *Evaluation of Alternate Water Gas Shift Configurations for IGCC Systems*, DOE/NETL-401/080509.

APPENDIX

A	cross-sectional area of packing bed (cm^2)
a	the stoichiometric coefficient for the complexation reaction
C_i	concentration of component i
$\overline{C_p}$	heat capacity of gas mixture (J/K·mol)
$\widetilde{C_{pi}}$	heat capacity of component i (J/K·mol)
$\widehat{C_{ps}}$	heat capacity of adsorbent (J/K·g)
C_v	valve flow coefficient
D	bed diameter (cm)
$D_{ax,i}$	axial dispersion coefficient (cm^2/s)
h	heat transfer coefficient (J/K·cm^2·s)
H_i	adsorption heat of component i (J/mole)
$\bar{k}$	average thermal conductivity (J/K·cm·s)
K_{LDF}	linear driving force coefficient (min^{-1})
k_c	the equilibrium constant for the chemisorption reaction(atm^{-1})
k_R	the equilibrium constant for the additional complexation reaction(atm^{-a})
n_i	adsorptive quantity on the solid phase of component i (mole/cm^3)
n_i^*	equilibrium adsorptive quantity on the solid phase of component i (mole/cm^3)
m	the saturation chemisorption capacity of the chemisorbent surface(mole/kg)
P	pressure (atm)
P_1	upstream pressure (atm)
P_2	downstream pressure (atm)

q	mole flow rate (mole/s)
q'	flow rate (L/min at 1atm, 273K)
R	gas constant (82.06 atm·cm3/gmol·K)
SG	specific gravity of gas
T	temperature (K)
T_∞	room temperature (K)
t	time (s)
y_i	mole fraction of component i in the gas phase (dimensionless)
z	axial coordinate (cm)
ε	bed porosity (dimensionless)
ρ_s	particle density (g/cm^3)